Available online at www.sciencedirect.com
SCIENCE DIRECT®
Journal of Solid State Chemistry 177 (2004) 3484–3489
JOURNAL OF SOLID STATE CHEMISTRY
http://elsevier.com/locate/jssc

Thermophysical properties of $SrHfO_3$ and $SrRuO_3$

Shinsuke Yamanaka,[a] Takuji Maekawa,[a] Hiroaki Muta,[a] Tetsushi Matsuda,[b] Shin-ichi Kobayashi,[b] and Ken Kurosaki[a,*]

[a] *Department of Nuclear Engineering, Graduate School of Engineering, Osaka University, Yamadaoka 2-1, Suita-shi, Osaka-fu 565-0871, Japan*
[b] *Nuclear Fuel Industries, Ltd., Ohaza-Noda 950, Kumatori-cho, Sennan-gun, Osaka 590-0481, Japan*

Received 4 March 2004; received in revised form 19 May 2004; accepted 19 May 2004

Available online 11 August 2004

Abstract

Polycrystalline samples of strontium series perovskite type oxides, $SrHfO_3$ and $SrRuO_3$ were prepared and the thermophysical properties were measured. The average linear thermal expansion coefficients are $1.13 \times 10^{-5}\,K^{-1}$ for $SrHfO_3$ and $1.03 \times 10^{-5}\,K^{-1}$ for $SrRuO_3$ in the temperature range between 423 and 1073 K. The melting temperatures T_m of $SrHfO_3$ and $SrRuO_3$ are 3200 and 2575 K, respectively. The longitudinal and shear sound velocities were measured by an ultrasonic pulse-echo method at room temperature in air, which enables to evaluate the elastic moduli and Debye temperature. The heat capacity was measured by using a differential scanning calorimeter, DSC in high-purity argon atmosphere. The thermal diffusivity was measured by a laser flash method in vacuum. The thermal conductivities of $SrHfO_3$ and $SrRuO_3$ at room temperature are 5.20 and $5.97\,W\,m^{-1}\,K^{-1}$, respectively.

Keywords: $SrHfO_3$; $SrRuO_3$; Perovskite; Thermal expansion coefficient; Melting temperature; Debye temperature; Heat capacity; Thermal conductivity; Thermal barrier coating

1. Introduction

The perovskite type oxides have potential to be attractive functional materials because they have various unique properties in spite of their relatively simple crystal structure. For example, $SrTiO_3$ is a typical perovskite dielectric material with a wide range of technological applications. Its special properties, such as ferroelectricity [1], semiconductivity [2], superconductivity [3], catalytic activity [4], and thermoelectricity [5], have been reported extensively.

Thermal barrier coatings (TBCs) of partly Y_2O_3 stabilized ZrO_2 (PYSZ) films are widely used to protect hot section parts of aircraft and land-based turbines by reducing the temperature of metal substrates. Their continued development is essential for improving the efficiency and performance of gas turbines by allowing the inlet gas temperature to be increased further. However this standard material has a limited temperature capability due to accelerated sintering and phase transformations at high temperatures. As a result, a world-wide effort has been undertaken to identify new candidates for a TBC application [6,7]. In general, TBC materials have to fulfill most of the following requirements, such as a stable phase, low thermal conductivity ($<2\,W\,m^{-1}\,K^{-1}$), high thermal expansion coefficient conductivity ($>9 \times 10^{-6}\,K^{-1}$), chemical resistance, low sintering rate and high fracture toughness.

$SrHfO_3$ has been well known for a long time, and it has a high melting temperature [8]. Recently, Kennedy et al. [9] investigated its high-temperature phase transitions using powder neutron diffraction. $SrRuO_3$ has an interesting magnetic system [10,11] and one of the highly conductive metallic oxides [12]. So, it has found use for electrodes and junctions in microelectronic devices. Up to now, many studies have done on the thin films of $SrRuO_3$ [13–15] at low temperatures.

We have systematically studied the thermophysical, mechanical, and thermoelectric properties of barium and strontium series perovskite type oxides, $BaUO_3$, $BaZrO_3$, $BaCeO_3$, $BaMoO_3$, $SrCeO_3$, and $SrZrO_3$

*Corresponding author. Fax: +81-6-6879-7889.
E-mail address: kurosaki@nucl.eng.osaka-u.ac.jp (K. Kurosaki).

0022-4596/$ - see front matter © 2004 Elsevier Inc. All rights reserved.
doi:10.1016/j.jssc.2004.05.039

[16–24]. In the present study, the thermophysical properties, viz. the thermal expansion coefficient, melting temperature, elastic moduli, Debye temperature, Vickers hardness, heat capacity, and thermal conductivity of $SrHfO_3$ and $SrRuO_3$ were measured. The relationships between the properties were studied.

2. Experimental procedure

The polycrystalline samples of $SrHfO_3$ and $SrRuO_3$ were prepared by mixing the appropriate amounts of HfO_2 (Furuuchi Chemical, 99.9%), RuO_2 (Rare Metallic, 99.9%), and $SrCO_3$ (Aldrich Chemical, 99.9+%), followed by reacting at 1273 K in air. After that, the $SrHfO_3$ sample was sintered at 1873 K for 10 h in air. On the other hand, the $SrRuO_3$ powder was placed into a 20 mm diameter graphite die and given a spark plasma sintering (SPS, SUMITOMO COAL MINING Dr Sinter SPS-1020 apparatus) at 1673 K for 1 min under nitrogen atmosphere. The powder X-ray diffraction (RIGAKU RINT2000) was performed at room temperature using Cu$K\alpha$ radiation. In order to determine the chemical composition, the SEM-EDX analysis was performed using HITACHI S-2600H SEM instrument equipped with the energy-dispersive HORIBA EX-200 system. The oxygen analysis was performed using HORIBA EMGA-550 to identify the oxygen concentration of the samples. For measurements of the thermophysical properties, appropriate shapes of the samples were cut from the sintered pellets. The bulk density of the samples was determined by the geometric measurement.

The high-temperature powder X-ray diffraction analysis was performed from room temperature to 1073 K to study the phase transition and thermal expansion behavior. The average linear thermal expansion coefficient was calculated in the temperature range from 300 to 1100 K. The melting temperature was measured by the thermal arrest method under a reducing atmosphere.

The longitudinal and shear sound velocities were measured by the ultrasonic pulse-echo method (NIHON MATECH Echometer 1062) at room temperature in air. The sintered sample was bonded to a 5 MHz longitudinal or shear sound wave echogenic transducer. From the sound velocities, the elastic moduli and Debye temperature were evaluated. The hardness was measured by loading a diamond pyramid-type (with apex 136°) indenter into the surface of the specimen at room temperature, using the micro-Vickers hardness tester (MATSUZAWA SEIKI MHT-1).

The specific heat capacities of $SrHfO_3$ and $SrRuO_3$ were measured by the differential scanning calorimeter (DSC, ULVAC) apparatus, in the temperature range from room temperature to about 1200 K. The apparatus has a "triple-cell" system and an adiabatic temperature control system, which was originally developed by Takahashi et al. [25]. The principle of the apparatus is briefly summarized in literature. The measurement was made out in high-purity argon (99.999%) atmosphere with a flow rate of 100 ml min^{-1}. The accuracy of the apparatus was checked using an alpha-Al_2O_3 standard.

The thermal diffusivities of $SrHfO_3$ and $SrRuO_3$ were measured by the laser flash method from room temperature to about 1000 K in vacuum (10^{-4} Pa) by using TC-7000 (ULVAC). The thermal diffusivity at a temperature obtained during the heating process also was checked during the cooling cycle.

The thermal conductivity was calculated from the thermal diffusivity α, heat capacity C_P, and density ρ, using the following standard expression:

$$\lambda = \alpha C_P \rho.$$

3. Results and discussion

The powder X-ray diffraction patterns at room temperature of the samples show that the orthorhombic [9,26] perovskite type single phase $SrHfO_3$ and $SrRuO_3$ are obtained in the present study. The lattice parameters of $SrHfO_3$ and $SrRuO_3$ evaluated from the X-ray diffraction pattern are $a = 0.5790$ nm, $b = 0.5851$ nm, $c = 0.8243$ nm and $a = 0.5569$ nm, $b = 0.5553$ nm, $c = 0.7874$ nm, respectively. The bulk densities of the samples are 94% of the X-ray density for $SrHfO_3$ and 97% of the X-ray density for $SrRuO_3$. The chemical composition of $SrHfO_3$ does not deviate from the stoichiometric composition. On the other hand, the estimated oxygen concentration in $SrRuO_3$ is slightly lower than the stoichiometric composition. The sample characteristics are summarized in Table 1. $SrHfO_3$ and $SrRuO_3$ show white and black color, respectively.

The conventional parameter describing the geometric distortion of the perovskite type compound is defined as a tolerance factor, t:

$$t = \frac{r_A + r_O}{\sqrt{2}(r_B + r_O)},$$

where r_A, r_B, r_O are the ionic radii of each atom. Ordinarily, the value of "t" is within 0.75–1.1 for the perovskite type oxides. The cubic structure has a value near 1. As the value of "t" shifts from 1, the geometric distortion becomes large. The value of the tolerance factor "t" of $SrHfO_3$ and $SrRuO_3$ are shown in Table 1. The Shannon's values of the ionic radius [27] are used in the present study.

Recently, Kennedy et al. and Chakoumakos et al. reported high-temperature phase transitions in $SrHfO_3$ and $SrRuO_3$ studied by using high-temperature neutron diffraction and the Rietveld method [9,28,29]. In these papers, it is reported that $SrHfO_3$ undergoes four phase

Table 1
Sample characteristics and thermophysical properties of $SrHfO_3$ and $SrRuO_3$

		$SrHfO_3$	$SrRuO_3$
Crystal system at RT		Orthorhombic	Orthorhombic
Lattice parameter at RT (nm)	a	0.579	0.557
	b	0.585	0.555
	c	0.824	0.787
Relative density (% TD)		94	97
Tolerance factor	t	0.958	1.001
Average linear thermal expansion coefficient (K^{-1})	α_l	1.13×10^{-5}(300–1100 K)	1.03×10^{-5}(300–1100 K)
Oxygen concentration	O/M	3.03	2.85
Longitudinal wave velocity ($m\,s^{-1}$)	V_L	6118	6312
Shear wave velocity ($m\,s^{-1}$)	V_S	3531	3083
Young's modulus (GPa)	E	220	161
Shear modulus (GPa)	G	87.9	60.1
Compressibility (GPa^{-1})	β	6.82×10^{-3}	5.83×10^{-3}
Debye temperature (K)	θ_D	490	448
Melting temperature (K)	T_m	3200	2575
Vickers hardness (GPa)	H_V	9.3	12.7
Heat capacity ($C_P=a+bT+cT^{-2}$) ($JK^{-1}mol^{-1}$)	a	118	108
	b	1.76×10^{-2}	2.65×10^{-2}
	c	-8.18×10^{5}	-5.19×10^{5}
Thermal conductivity at RT ($W\,m^{-1}\,K^{-1}$)	λ	4.54	5.72

transitions: orthorhombic ($Pbnm$)→orthorhombic ($Cmcm$)→tetragonal ($I4/mcm$)→cubic ($Pm\bar{3}m$), $SrRuO_3$ undergoes three phase transitions: orthorhombic ($Pbnm$)→tetragonal ($I4/mcm$)→cubic ($Pm\bar{3}m$).

In the present study, the phase transitions in $SrHfO_3$ and $SrRuO_3$ are observed from the high-temperature X-ray diffraction analysis. $SrHfO_3$ and $SrRuO_3$ undergo following phase transitions:$SrHfO_3$:

$$\text{Orthorhombic } (Pbnm) \xrightarrow[800\,K]{} \text{Orthorhombic } (Cmcm) \xrightarrow[1000\,K]{} \text{tetragonal } (I4/mcm),$$

$SrRuO_3$:

$$\text{Orthorhombic } (Pbnm) \xrightarrow[800\,K]{} \text{tetragonal } (I4/mcm) \xrightarrow[950\,K]{} \text{Cubic } (Pm3m).$$

These results well agree with literature data [9,29].

From the high-temperature X-ray analysis, the temperature dependences of lattice parameters (nm) of $SrHfO_3$ and $SrRuO_3$ are obtained as follows:

$SrHfO_3$, 300–800 K, orthorhombic ($Pbnm$):

$$a = 5.68\times10^{-1} + 6.00\times10^{-5}T - 9.53\times10^{-8}T^2 + 6.36\times10^{-11}T^3,$$

$$b = 5.67\times10^{-1} + 6.00\times10^{-5}T - 6.90\times10^{-8}T^2 + 2.85\times10^{-11}T^3,$$

$$c = 8.15\times10^{-1} - 1.00\times10^{-5}T + 1.18\times10^{-8}T^2,$$

$SrHfO_3$, 800–1000 K, orthorhombic ($Cmcm$):

$$a = 1.61\times10^{-1} + 2.20\times10^{-3}T - 2.43\times10^{-6}T^2 + 8.95\times10^{-10}T^3,$$

$$b = -4.79\times10^{-1} + 4.51\times10^{-3}T - 5.20\times10^{-6}T^2 + 1.99\times10^{-9}T^3,$$

$$c = -4.37\times10^{-1} + 4.26\times10^{-3}T - 4.80\times10^{-6}T^2 + 1.81\times10^{-9}T^3,$$

$SrHfO_3$, 1000–1100 K, tetragonal ($I4/mcm$):

$$a = -5.70\times10^{-1} + 4.18\times10^{-3}T - 4.84\times10^{-6}T^2 + 1.82\times10^{-9}T^3,$$

$$c = -3.90\times10^{-1} + 4.27\times10^{-3}T - 4.82\times10^{-6}T^2 + 1.77\times10^{-9}T^3,$$

$SrRuO_3$, 300–800 K, orthorhombic ($Pbnm$):

$$a = 5.56\times10^{-1} + 2.15\times10^{-6}T + 3.58\times10^{-9}T^2,$$

$$b = 5.54\times10^{-1} - 7.93\times10^{-6}T + 3.04\times10^{-8}T^2 - 1.81\times10^{-11}T^3,$$

$$c = 7.88\times10^{-1} - 2.00\times10^{-5}T + 5.07\times10^{-8}T^2 - 3.30\times10^{-11}T^3,$$

$SrRuO_3$, 800–950 K, tetragonal ($I4/mcm$):

$$a = 5.34\times10^{-1} + 3.00\times10^{-5}T + 2.61\times10^{-8}T^2 - 2.96\times10^{-11}T^3,$$

$$c = 8.57\times10^{-1} - 5.00\times10^{-5}T - 1.54\times10^{-7}T^2 + 1.47\times10^{-10}T^3,$$

$SrRuO_3$, 950–1100 K, cubic ($Pm3m$):

$$a = 3.31 \times 10^{-1} + 1.80 \times 10^{-4} T - 1.69 \times 10^{-7} T^2 + 5.52 \times 10^{-11} T^3,$$

where T is in Kelvin. The temperature dependences of lattice volume (nm^3) are as follows:

$SrHfO_3$, 300–1100 K:

$$V = 6.66 \times 10^{-2} + 5.76 \times 10^{-6} T - 4.49 \times 10^{-9} T^2 + 1.93 \times 10^{-12} T^3,$$

$SrRuO_3$, 300–1100 K:

$$V = 5.98 \times 10^{-2} + 3.13 \times 10^{-6} T - 2.04 \times 10^{-9} T^2 + 1.13 \times 10^{-12} T^3,$$

where T is in Kelvin. The temperature dependences of linear thermal expansion coefficients α_l (K^{-1}) of $SrHfO_3$ and $SrRuO_3$ measured by the high-temperature X-ray diffraction are as follows:

$SrHfO_3$, 300–1100 K:

$$\alpha_l = 3.88 \times 10^{-6} + 1.75 \times 10^{-8} T - 9.49 \times 10^{-12} T^2,$$

$SrRuO_3$, 300–1100 K:

$$\alpha_l = -4.16 \times 10^{-6} + 5.86 \times 10^{-8} T - 7.78 \times 10^{-11} T^2 + 3.41 \times 10^{-14} T^3,$$

where T is in Kelvin. The average linear thermal expansion coefficients α_l are $1.13 \times 10^{-5}\,K^{-1}$ for $SrHfO_3$ and $1.03 \times 10^{-5}\,K^{-1}$ for $SrRuO_3$ in the temperature range between 300 and 1100 K.

The melting temperature T_m of $SrHfO_3$ and $SrRuO_3$ is shown in Table 1. The values are 3200 K for $SrHfO_3$ and 2575 K for $SrRuO_3$. The melting temperature of $SrHfO_3$ and $SrRuO_3$ is in good agreement with literature data [8,30]. The melting temperature of $SrHfO_3$ is higher than that of other perovskites, for example, the melting temperature of $SrTiO_3$ is 2170 K [31], and that of $SrZrO_3$ is 2883 K [24].

The relationship between the linear thermal expansion coefficient and melting temperature for the perovskite oxides is shown in Fig. 1. In this figure, the data of other perovskite type oxides are plotted for comparison [16,17,19,24,31]. It is confirmed that the linear thermal expansion coefficient varies inversely as the melting temperature for many substances [32]. For the barium and strontium series perovskite type oxides, the products of α_l and T_m show approximately the same value (=0.022).

For an isotropic medium, the Young's modulus E, shear modulus G, compressibility β, and Debye temperature θ_D can be written in terms of the longitudinal sound velocity V_L and shear sound velocities V_S as follows [33,34]:

$$E = \frac{\rho V_S^2 (3V_L^2 - 4V_S^2)}{(V_L^2 - V_S^2)},$$

$$G = \rho V_S^2,$$

$$\beta = \frac{1}{\rho (V_L^2 - \frac{4}{3} V_S^2)},$$

$$\theta_D = \left(\frac{h}{k_B}\right)\left[\frac{9N}{4\pi V (V_L^{-3} + 2V_S^{-3})}\right]^{\frac{1}{3}},$$

where h is the Plank constant, k_B is the Boltzmann constant, N is the number of atoms in a unit cell, and V is the unit cell volume. The elastic moduli and Debye temperature evaluated in the present study are summarized in Table 1. The Vickers hardness is shown in Table 1. In the present study, the applied load and loading time were chosen to be 1 kg (9.8 N) and 30 s. The measurement was repeated 10 times for a sample, and the average value was calculated from the data in which the maximum and minimum values were excluded.

The Debye temperature θ_D can be related to the melting temperature T_m in K, the molar mass M, and the molar volume V_m by the Lindemann relationship [35]. The relationships have been reexamined for the perovskite type oxides, and the ratio of θ_D to $q^{5/6}(T_m/(MV_m^{2/3}))^{1/2}$ has been evaluated to be 1.60 [36]. Fig. 2 shows this relationship for $SrHfO_3$ and $SrRuO_3$, together with the data of other substances [17,24]. The proportionality constant of $SrHfO_3$ and $SrRuO_3$ is almost identical (around 1.60), indicating typical characteristics of the perovskite type oxides.

The temperature dependence of the heat capacity of $SrHfO_3$ and $SrRuO_3$ determined by the scanning

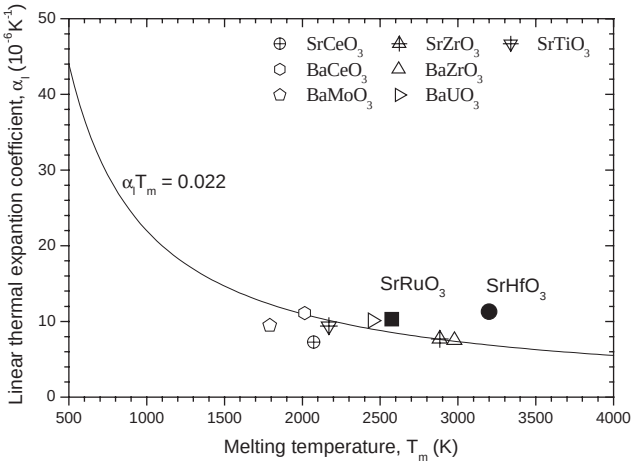

Fig. 1. Relationship between the linear thermal expansion coefficient α_l and melting temperature T_m for $SrHfO_3$ and $SrRuO_3$, together with the data of other perovskites [16,17,19,24,30].

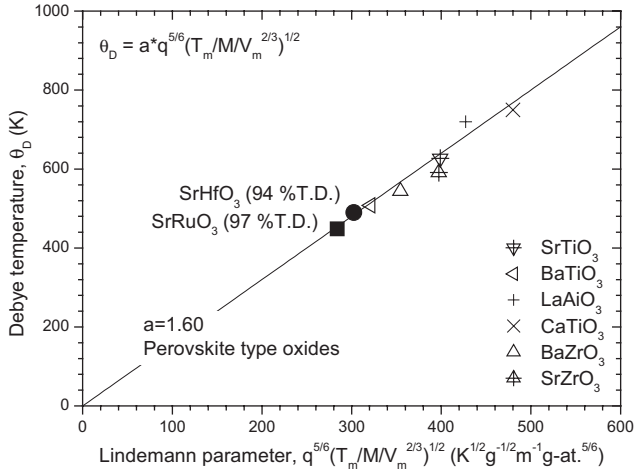

Fig. 2. Relationship between the Debye temperature and Lindemann parameter for $SrHfO_3$ and $SrRuO_3$, together with the data of other perovskites [17,24].

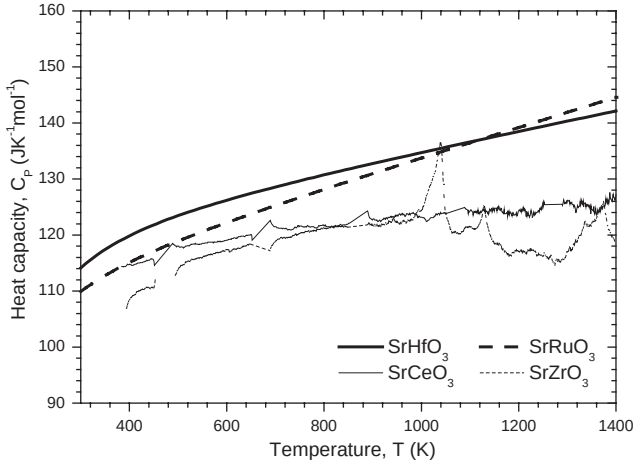

Fig. 3. Temperature dependence of the heat capacities for $SrHfO_3$ and $SrRuO_3$, together with the data of other perovskites [17,18].

method is shown in Fig. 3, together with the data of other substance [17,18]. In the temperature range between 300 and 1300 K, the empirical equation for the C_P of $SrHfO_3$ is determined from the experimental data as follows:

$$C_P(\mathrm{JK^{-1}\,mol^{-1}}) = 118 + 1.76\times10^{-2}T - 8.18\times10^{5}/T^{2}.$$

On the other hand, the empirical equation for the C_P of $SrRuO_3$ is determined from the experimental values as follows:

$$C_P(\mathrm{JK^{-1}\,mol^{-1}}) = 108 + 2.65\times10^{-2}T - 5.19\times10^{5}/T^{2}.$$

The peaks from the phase transitions are not observed in the C_P curves of $SrHfO_3$ and $SrRuO_3$.

The temperature dependence of the thermal conductivity of $SrHfO_3$ and $SrRuO_3$ is shown in Fig. 4, together

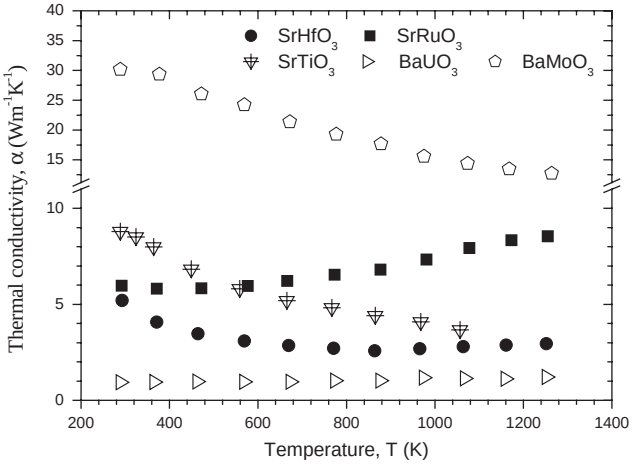

Fig. 4. Temperature dependence of the thermal conductivities for $SrHfO_3$ and $SrRuO_3$, together with the data of other perovskites [20,22,23].

with the data of other substances [20,22,23]. The thermal conductivity was corrected to 100% of the theoretical density by using Schulz's equation [37]. The thermal conductivity of $SrHfO_3$ decreases with increasing temperature, which indicates that the phonon conduction is predominant. On the other hand, the thermal conductivity of $SrRuO_3$ increases with increasing temperature, which indicates that the electronic contribution is predominant. The thermal conductivities of $SrHfO_3$ and $SrRuO_3$ at room temperature are 5.20 and 5.97 $\mathrm{W\,m^{-1}\,K^{-1}}$, respectively. These values are too high to utilize these materials for TBC application. The value of better TBC materials should have much lower thermal conductivity ($<2\,\mathrm{W\,m^{-1}\,K^{-1}}$).

4. Conclusion

The polycrystalline high-density samples of strontium series perovskite type oxides, $SrHfO_3$ and $SrRuO_3$ were prepared. The thermophysical properties of $SrHfO_3$ and $SrRuO_3$ were measured and the relationships between the properties were studied. It is confirmed that the linear thermal expansion coefficient varies inversely as the melting temperature. The Young's moduli of $SrHfO_3$ and $SrRuO_3$ are 220 and 161 GPa, respectively. The Vickers hardness of $SrHfO_3$ and $SrRuO_3$ are 9.3 and 12.7 GPa, respectively. In the temperature range between 300 and 1300 K, the empirical equation for the C_P of $SrHfO_3$ and $SrRuO_3$ is determined as follows:

$$C_P(\mathrm{JK^{-1}\,mol^{-1}}) = 118 + 1.76\times10^{-2}T - 8.18\times10^{5}/T^{2}(\mathrm{SrHfO_3}),$$

$$C_P(\mathrm{JK^{-1}\,mol^{-1}}) = 108 + 2.65\times10^{-2}T - 5.19\times10^{5}/T^{2}(\mathrm{SrRuO_3}).$$

The thermal conductivities of $SrHfO_3$ and $SrRuO_3$ at room temperature are 5.20 and 5.97 $W m^{-1} K^{-1}$, respectively.

References

[1] J.G. Bednorz, K.A. Muller, Phys. Rev. Lett. 52 (1984) 2289.
[2] H.P.R. Frederikse, W.R. Thurber, W.R. Hosler, Phys. Rev. 134 (1964) A442.
[3] C.S. Koonce, M.L. Cohen, J.F. Schooley, W.R. Hosler, E.R. Pfeiffer, Phys. Rev. 163 (1967) 380.
[4] V.E. Henrich, Rep. Prog. Phys. 48 (1985) 1481.
[5] H. Muta, K. Kurosaki, S. Yamanaka, J. Alloys Compds. 350 (2003) 292.
[6] K. Matsumoto, Y. Itoh, T. Kameda, Sci. Technol. Adv. Mater. 4 (2003) 153.
[7] H.M. Wang, M.C. Simmonds, J.M. Rodenburg, Mater. Chem. Phys. 77 (2003) 802.
[8] M.P. Jorba, G. Tilloca, R. Collongues, Int. Symp. Magnetohydrodyn. Electric Power Generation 3 (1964) 1185.
[9] B.J. Kennedy, C.J. Howard, B.C. Chakoumakos, Phys. Rev. B 60 (1999) 2972.
[10] D. Kim, B.L. Zink, F. Hellman, S. McCall, G. Cao, J.E. Crow, Phys. Rev. B 67 (2003) 100406.
[11] D. Kirillov, Y. Suzuki, L. Antognazza, K. Char, I. Bozovic, T.H. Geballe, Phys. Rev. B 51 (1995) 12825.
[12] C.L. Chen, Y. Cao, Z.J. Huang, Q.D. Jiang, Z. Zhang, Y.Y. Sun, W.N. Kang, L.M. Dezaneti, W.K. Chu, C.W. Chu, Appl. Phys. Lett. 71 (1997) 1047.
[13] X. Fang, T. Kobayashi, J. Appl. Phys. 90 (2001) 161.
[14] J.J. Neumeier, A.L. Cornelius, K. Andres, Phys. Rev. B 64 (2001) 172406.
[15] F. Castelpoggi, L. Morelli, H.R. Salva, S.L. Cuffini, R. Carbonio, R.D. Sanchez, Solid State Commun. 101 (1997) 597.
[16] S. Yamanaka, M. Fujikane, T. Hamaguchi, H. Muta, T. Oyama, T. Matsuda, S. Kobayashi, K. Kurosaki, J. Alloys Compds. 359 (2003) 109.
[17] S. Yamanaka, K. Kurosaki, T. Matsuda, S. Kobayashi, J. Alloys Compds. 352 (2003) 52.
[18] T. Matsuda, S. Yamanaka, K. Kurosaki, S. Kobayashi, J. Alloys Compds. 351 (2003) 43.
[19] S. Yamanaka, T. Matsuda, K. Kurosaki, M. Uno, J. Nucl. Sci. Technol. (Suppl. 3) (2002) 709.
[20] K. Kurosaki, T. Matsuda, M. Uno, S. Kobayashi, S. Yamanaka, J. Alloys Compds. 319 (2001) 271.
[21] S. Yamanaka, K. Kurosaki, T. Matsuda, M. Uno, J. Nucl. Mater. 294 (2001) 99.
[22] H. Muta, K. Kurosaki, S. Yamanaka, Thermoelectric properties of doped $BaTiO_3$–$SrTiO_3$ solid solution, J. Alloys Compds. 368 (2004) 22.
[23] K. Kurosaki, T. Oyama, H. Muta, M. Uno, S. Yamanaka, Thermoelectric properties of perovskite type barium molybdate, J. Alloys Compds. 372 (2004) 65.
[24] S. Yamanaka, K. Kurosaki, T. Matsuda, T. Oyama, H. Muta, S. Kobayashi, M. Uno, Thermophysical properties of perovskite type strontium cerate and zirconate, J. Am. Ceram. Soc., submitted for publication.
[25] Y. Takahashi, M. Asou, Thermochim. Acta 223 (1993) 7.
[26] B.J. Kennedy, B.A. Hunter, J.R. Hester, Phys. Rev. B 65 (2002) 224103.
[27] R.D. Shannon, Acta Crystallogr. A 32 (1976) 751.
[28] B.C. Chakoumakos, S.E. Nagler, S.T. Misture, H.M. Christen, Physica B 241–243 (1998) 358.
[29] B.J. Kennedy, B.A. Hunter, Phys. Rev. B 58 (1998) 653.
[30] N.D. Zhigadlo, P. Odier, J.Ch. Marty, P. Bordet, A. Sulpice, Physica C 387 (2003) 347.
[31] N. Sata, Solid State Ion. 97 (1997) 437.
[32] L.G. Van Uitert, et al., Mater. Res. Bull. 12 (1977) 261.
[33] K. Yamada, S. Yamanaka, M. Katsura, Tech. Rep. Osaka Univ. 47 (1997) 181.
[34] M. Fukuhara, I. Yamauchi, J. Mater. Sci. 28 (1993) 4681.
[35] F.A. Lindemann, Phys. Z. 14 (1910) 609.
[36] The Chemical Society of Japan (Ed.), Kikan Kagaku Sousetsu, Perovskite-Related Compds. 32 (1997) 37.
[37] B. Schulz, High Temp.-High Press. 13 (1981) 649.